Testing the Expanding Plasmon Model in the Galactic Center's Black Hole

August 27, 2011

Nara Higano[1]
University of California, Los Angeles
Physics and Astronomy REU

Abstract

We investigate the temporal behavior of flares in the NIR and millimeter regime of Sagittarius A*, the supermassive black hole in the Galactic center, observed on 2005 July 31 at the Keck II telescope, the Very Large Telescope, and the Submillimeter Array. The time lags between a VLT NIR flare and SMA millimeter flare as well as between three quasi-simultaneous Keck NIR flares are quantified through application of the z-transform discrete cross correlation function. Through this analysis, we contribute a new value of approximately 160 minutes to the collection of NIR-mm time lag estimates and eliminate the previous outlying estimate of 20 minutes. Due to insignificant time lag estimates between inter-NIR flares, the validity of the expanding synchrotron plasmon model cannot be satisfactorily tested with current observations. We show that significant inter-NIR time lags can in principle be achieved by decreasing light curve sampling intervals.

1 Introduction

The radio, IR, millimeter, and X-ray source Sagittarius A* is identified with a supermassive black hole ($3.7 \times 10^6 M_\odot$) at the center of our galaxy (Baganoff et al. 2001; Genzel et al. 2003; Schoedel et al. 2003; Ghez et al. 2003, 2004, 2005a). Observations of the flare behavior of Sgr A* in these wavelengths indicate that this source is highly variable. Because of the flares' hour-timescales at IR and millimeter wavelengths, it is likely that these flares originate from near the black hole's event horizon (Ghez et al. 2004; Mauerhan et al. 2005; Herrnstein et al. 2004). Further investigation into Sgr A*'s flare activity may elucidate details about the environs of the black hole and its accretion disk

[1]Gustavus Adolphus College, Saint Peter, MN 56082

(Marrone et al. 2008). Several current models propose a variety of mechanisms that explain the energetic emission processes of these flares. Yet few models exist that explain the temporal development of flares at different wavelengths. As well, previous studies have often been limited in their analysis of the temporal development of flares at different wavelengths simply due to a lack of complementary observations (Eckart et al. 2004, 2006c; Yusef-Zadeh et al. 2006b). Thus analysis was often restricted to details offered by an individual flare (Marrone et al. 2008).

The expanding plasmon model seeks to explain the temporal development of flares at different wavelengths. This model proposes that hot plasmon in the accretion disk cools adiabatically as it expands (van der Laan 1966). Under this scheme, the plasmon is a source of synchrotron radiation that is initially optically thick, but during expansion it becomes optically thin at continuously longer wavelengths.

Here, we examine the time-evolution of several observed NIR flares and a corresponding millimeter flare obtained from the Keck II telescope, the Very Large Telescope, and the Submillimeter Array (§2). We investigate the quantitative time lags between inter-NIR flares as well as NIR-mm flares (§3.1), and in a preliminary effort to better understand the environment of Sgr A*, we use the expanding plasmon model to compare the projected and observed time lags between flares at different wavelengths (§3.2).

2 Observations and Reductions

The data presented here were obtained from three observatories that monitored the Galactic center on 2005 July 30-31 (UT). We report on four flares observed at NIR wavelengths and one flare observed at millimeter wavelength. Observation details are discussed in the following sections.

2.1 Near-Infrared Data

2.1.1 Keck Observations

The W. M. Keck II 10-meter telescope observed Sgr A* on the night of 2005 July 31 in the H ($\lambda_0 = 1.63\mu m$, $\Delta\lambda = 0.30\mu m$), K' ($\lambda_0 = 2.12\mu m$, $\Delta\lambda = 0.35\mu m$), and L' ($\lambda_0 = 3.78\mu m$, $\Delta\lambda = 0.70\mu m$) photometric bands using the NIRC2 (PI: K. Matthews) near-infrared camera and the laser guide star adaptive optics system (Wizinowich et al. 2006; van Dam et al. 2006). Observations were made by cycling through the H, K', and L' filters for 113 minutes, with a three-filter cycle completed approximately every 210 seconds. Seeing on the night of July 31 was excellent, with resolution of 62-65 mas (FWHM) achieved at H and K' and 80-82 mas achieved at L'. See Figure 1 for the Keck NIR light curves. The reader is referred to Hornstein et al. (2007) for additional details.

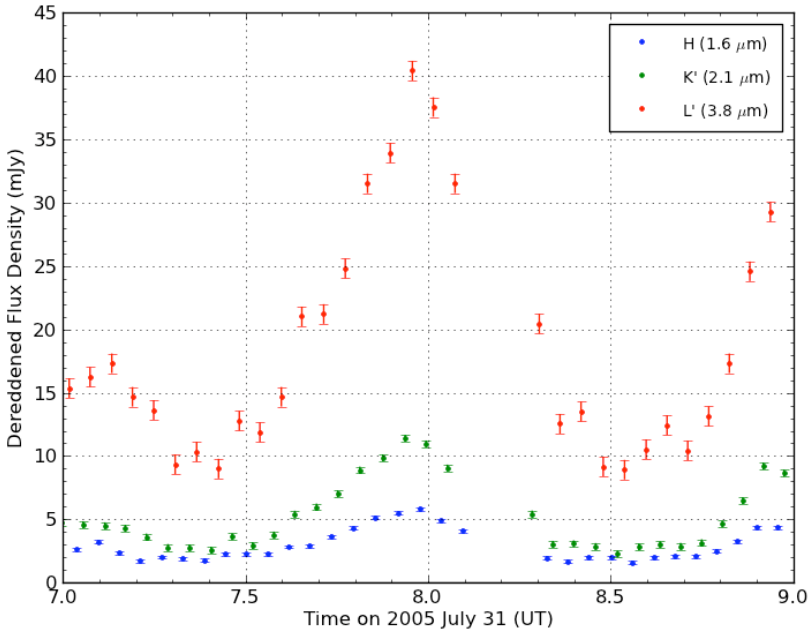

Figure 1: NIR light curves for Sgr A* on 2005 July 31 from Keck (*H*, *lower curve*; *K'*, *middle curve*; *L'*, *upper curve*). Three distinct flare events are detected at each photometric band.

2.1.2 VLT Observations

VLT observed Sgr A* on the night of 2005 July 30-31 in the *K'* band for nearly 8 hours using the natural guide star adaptive optics system and NIR camera NACO on UT4.[2] This observation directly precedes the Keck observation. The seeing conditions ranged between 1.0"-2.5" during the first two hours and 0.5"-1.25" thereafter. See Figure 2 for the VLT NIR light curve. The reader is referred to Meyer et al. (2008) for additional details.

2.1.3 NIR Data Reduction

The Galactic center Keck and VLT data have been reduced homogeneously. The Keck group utilizes PSF fitting without deconvolution, whereas the VLT groups use deconvolution and aperture photometry. Different dereddening factors and calibration values were used by the two groups, but through use of a multiplicative scaling factor on the Keck light curve, both data reduction methods were found to be consistent with each other. The reader is again referred to Meyer et al. (2008) for additional details.

[2]ESO program 075.B-0093(B).

2.2 SMA Millimeter Data

The SMA observed Sgr A* on the night of July 31 at 1.32 mm wavelength for approximately 6 hours. Seven antennas were used in the SMA "compact-north" configuration. During the observations, the zenith opacity ranged between 0.05-0.08. See Figure 2 for the SMA millimeter light curve. The reader is referred to Marrone et al. 2008 for additional details.

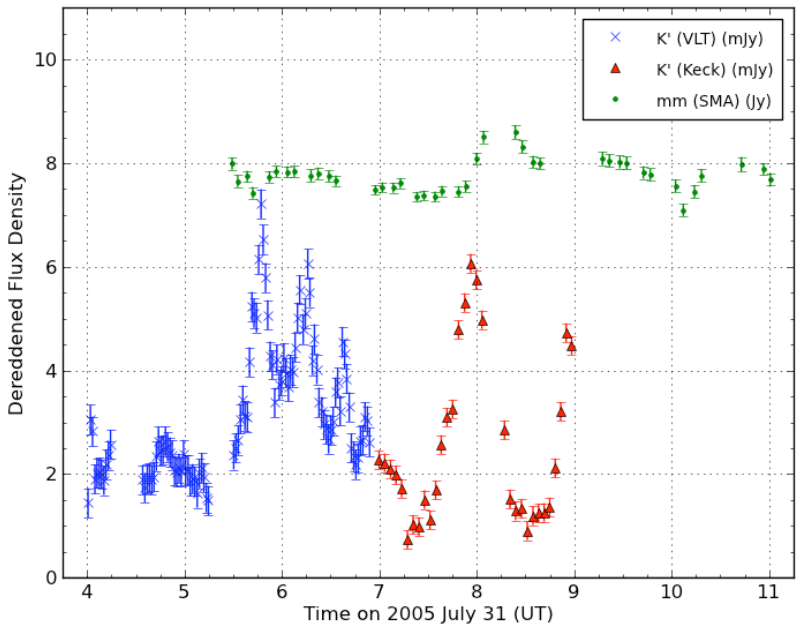

Figure 2: NIR (*K'*, *lower curve*) and millimeter (1.3 mm, *upper curve*) light curves for Sgr A* on 2005 July 31 from VLT, Keck, and the SMA. The flux units are mJy for the NIR and Jy for the millimeter data. Note that the millimeter data have been shifted upward by 3.5 Jy for better comparison.

3 Analysis and Results

3.1 Cross Correlation Analysis

3.1.1 The z-Transform Discrete Cross Correlation Function Method

The cross-correlation function (CCF) is a standard technique use to quantify time lags between light curves at different wavelengths. The CCF method assumes that the light curves are uniformly sampled. However, in most cases the light curves are sampled discretely at unequal intervals. In general, there exist three approaches for dealing with the uneven sampling of light curves: the interpolated cross correlation function (ICCF) (Gaskell and Peterson 1987);

the discrete correlation function (DCF) (Edelson and Krolik 1988); and the z-transform discrete cross correlation function (ZDCF) (Alexander 1997).

The ICCF method uses linear interpolation to compute the missing light curve data. It averages the cross correlation obtained by pairing the observed $a(t_i)$ with the interpolated value $b(t_i - \tau)$ and the cross correlation obtained by pairing the observed $b(t_j)$ with the interpolated value $a(t_j + \tau)$, where a and b are the two light curves and τ is the time lag. This method is unreliable if the light curves are undersampled because it assumes that the light curve varies smoothly. As well, it does not provide error estimates on the calculated cross correlation which are necessary for modeling.

The DCF method uses a binning procedure which orders all pairs of points from a and b according to τ in order to to approximate the missing data. The data are binned by equal width $\Delta\tau$. The bin average is used to estimate the cross correlation, and the bin's standard deviation is used to estimate the error.

The ZDCF method is an improved binning procedure with two major changes. First, the data are binned by equal population rather than equal width $\Delta\tau$. Second, a z-transform is used to calculate more accurate sampling errors. In practice it has been shown that the ZDCF is more robust than the ICCF and DCF in analysis of non-uniformly and sparsely sampled light curves. The time lag provided by both the ICCF and the DCF is characterized by τ_{peak} (the time lag at which the correlation coefficient is highest), while the ZDCF time lag is characterized by the centroid τ_{cent} (computed using all points between 0.8-1.0 of the maximum correlation coefficient). It has been found that τ_{peak} is much less stable than τ_{cent}. Additionally, the ZDCF method determines the error estimates of calculated time lags with a large number of Monte Carlo simulations. However, it has been shown through simulations that the ZDCF consistently overestimates time lag errors by a factor of as large as 1.4. We utilize the ZDCF method in this work.

3.1.2 NIR-millimeter Time Lags

A multitude of NIR-mm time lag values have been previously reported (see Table 1). As described in Meyer et al. (2008), the outlying 20 minute time lag report results from an uncertain correlation between the SMA millimeter and Keck NIR data. As these authors suggest, there also exists a possible correlation between the SMA millimeter and VLT NIR data with a visually inferred time lag of approximately 140 minutes. This correlation's inferred lag is much more congruous with previous reports than the original correlation's calculated 20 minute lag. We have performed the first ever cross correlation between the SMA and VLT data, with a resulting NIR-mm time lag estimate of 158.4 +3.6 -3.2 minutes. In Figure 3 we show the cross correlation of the VLT/Keck NIR and the SMA millimeter light curves. This more consistent estimate indicates that the previous uncertain correlation between the Keck and SMA flares is in fact a false correlation. Rather, the SMA flare is linked with the VLT flare, and the 158.4 minute lag estimate replaces the 20 minute lag estimate.

Table 1: Current reports on the NIR-millimeter time lag delay. (References: [1] Eckart et al. (2006a), [2] Eckart et al. (2009), [3] Yusef-Zadeh et al. (2006a), [4] Marrone et al. (2008), [5] Yusef-Zadeh et al. (2008), [6] Yusef-Zadeh et al. (2009), [7] Eckart et al. (2008b), [8] Trap et al. (2011), [9] this work.)

References	Date	mm wavelength	Time Lag (min)
1, 2.....	2004 Jul. 7	890 μm	< 120
3.....	2004 Sep. 3	850 μm	160
4, 5, 6...	2006 Jul. 17	1.3 mm/850 μm	100
6.....	2007 Apr. 5	1.3 mm	160
7.....	2008 Jun. 3	870 μm	90
8.....	2009 Apr. 1	870 μm	200
4.....	2005 Jul. 31	1.3 mm	20
9.....	2005 Jul. 31	1.3 mm	158.4

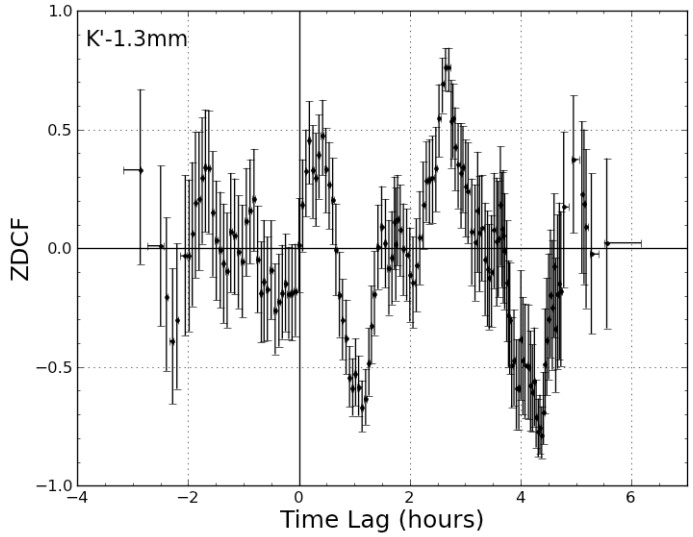

Figure 3: ZDCF correlation between Keck/VLT NIR (*K'*) and SMA millimeter (1.3 mm) light curves.

3.1.3 Inter-NIR Time Lags

There have been few studies that characterize the time lag between NIR bands. In this work, we determine the time lag between the Keck *H*, *K'*, and *L'* bands to be: 1.07 +1.56 -1.70 minutes (*H-K'*); 1.19 ± 1.53 minutes (*K'-L'*); and 2.27 +1.60 -3.13 minutes (*H-L'*). In Figure 4 we show the cross correlations of these NIR band combinations. As evident from the time lag errors, the correlations of the inter-NIR light curves show no evidence for significant time lags.

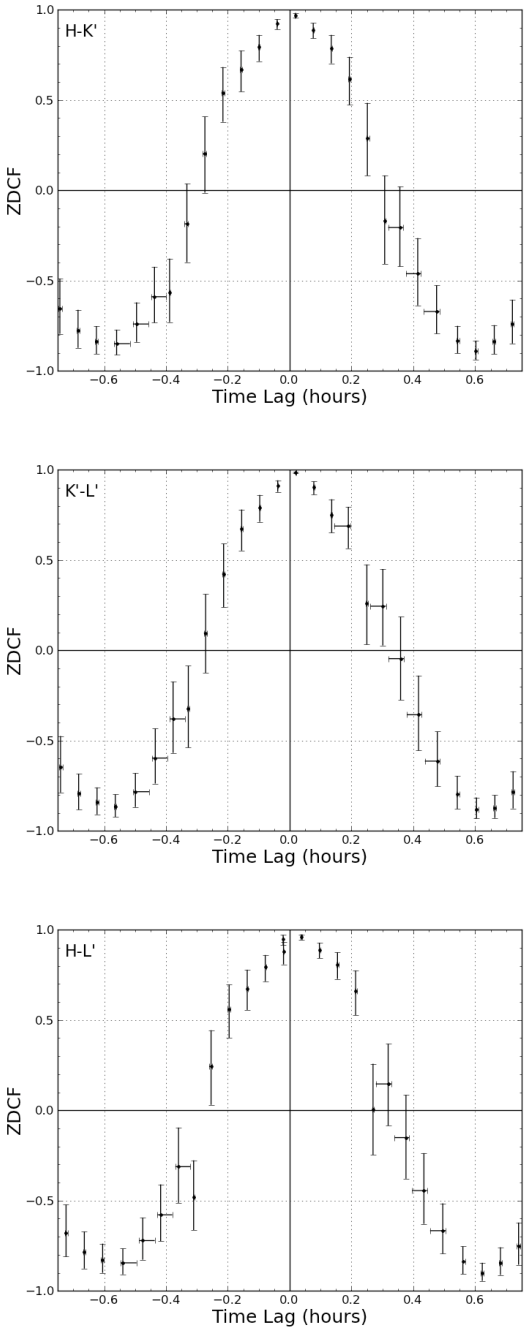

Figure 4: ZDCF correlations between each combination of inter-NIR light curves.

3.1.4 An Investigation of Inter-NIR Time Lag Errors

Various methods were explored to account for the relatively large inter-NIR time lag errors. First, the effect of the ZDCF error overestimation was investigated. The time lag errors were scaled by the overestimation factor of 1.4. However, when the errors are scaled, the mean values are only marginally significant. In Table 2, we show the scaled errors.

Second, the effect of the light curve flux error was investigated. The flux error on each light curve was reduced by a factor of $\frac{1}{3}$. This reduction had little effect on the time lag errors (see Table 2), indicating that the signal-to-noise ratio on the light curve observations has a negligible role in determining the error estimates.

Third, the effect of the light curve sampling intervals was investigated. More abundantly sampled *H* and *L'* light curves were simulated by linearly interpolating the *H* and *L'* flux values for the original sampling times of the *H*, *K'*, and *L'* light curves. While approximately 210 seconds were required to complete the original three-filter cycle, only approximately 140 seconds are required to complete the simulated two-filter cycle. When the sampling intervals of the light curves were decreased, the time lag errors were consequently also decreased (see Table 2).

Table 2: Various methods of investigating the inter-NIR time lag and errors.

Method	*H*-*K'* Lag (min)	*K'*-*L'* Lag (min)	*H*-*L'* Lag (min)
Original Light Curves	1.07	1.19	2.27
	1σ: +1.56 -1.70	1σ: ± 1.53	1σ: +1.60 -3.13
	3σ: +5.12 -6.17	3σ: +3.32 -3.33	3σ: +5.98 -6.68
Scaled Lag Error	1.07	1.19	2.27
	1σ: +1.11 -1.21	1σ: ± 1.09	1σ: +1.14 -2.24
	3σ: +3.66 -4.41	3σ: +2.37 -2.38	3σ: +4.27 -4.77
Flux Error Reduction	1.07	1.19	2.27
	1σ: +1.54 -1.60	1σ: ± 1.53	1σ: +1.57 -2.50
Simulated Light Curves	—	—	1.17
	—	—	1σ: +1.31 -1.06
	—	—	3σ: +4.40 -3.72

3.2 Expanding Plasmon Model Projections

It has been proposed that the temporal activity of the observed flares of Sgr A* could be explained in an expanding synchrotron plasmon model, as formulated by van der Laan (1966). In this model the electrons in the plasmon cool adiabatically, and the magnetic field is reduced while flux is conserved. These fundamental characteristics provide the non-radiative decreases in synchrotron radiation that we observe. This model predicts that a flare at one wavelength

will be associated with a later flare at longer wavelength. The activity of two distinct flares can be related through the frequency-time relationship of the plasmon model. If the peak of the first observed flare at frequency ν_1 occurs at time t_1, then the peak of the second observed flare at frequency ν_2 occurs at time

$$t_2 = (\beta t_0 + t_1)(\frac{\nu_1}{\nu_2})^{\frac{\gamma+4}{\beta(4\gamma+6)}} - \beta t_0, \quad (1)$$

where $\beta = 1$ (parameter for constant expansion velocity), $\gamma = 2.2$ (electron spectral index, as determined by Marrone et al. 2008), and t_0 corresponds to the "apparent age" of the expanding source.

This model can be tested by examining the projected outputs of the frequency-time relationship. When the time lag between two flares is known, the value for t_0 is inferred, and thus the time lag between two desired frequencies can be calculated.

Using this method, we have used the NIR-mm time lag value (with 3σ errors) to project an expected *H-L'* time lag range of approximately 4-5 minutes (see Table 3). This projected range is consistent with the original correlation (within 3σ error) between the Keck *H* and *L'* light curves. As well, much of the projected range is significant within the 3σ errors of the simulated *H* and *L'* light curves. Similarly we have used the inter-NIR time lag values to project expected NIR-mm time lag ranges (see Table 3). However, because the errors on the inter-NIR time lags are insignificantly large, the projected ranges are correspondingly broad.

Table 3: Projected time lag ranges.

Project to:	Project from:	Lower Bound (min)	Upper Bound (min)
H-L'	NIR-mm	4.07	4.89
NIR-mm	*H-K'*	-679.7	826.1
	K'-L'	-107.9	227.1
	H-L'	-162.4	303.4

4 Discussion and Conclusions

In this work, we investigate the temporal behavior of flares of Sgr A* observed on 2005 July 31 in the NIR and millimeter wavelengths. We correlate the VLT flare in the NIR regime to the SMA flare in the millimeter regime with a time lag of 158.4 minutes, a value that agrees well with previous NIR-mm lag reports. This link between the VLT and SMA flares replaces the previous false correlation between the SMA flare and the Keck flare in the NIR regime with a time lag of 20 minutes (the largest current outlier). In Figure 5, we have visually summarized the current NIR-mm time lag reports.

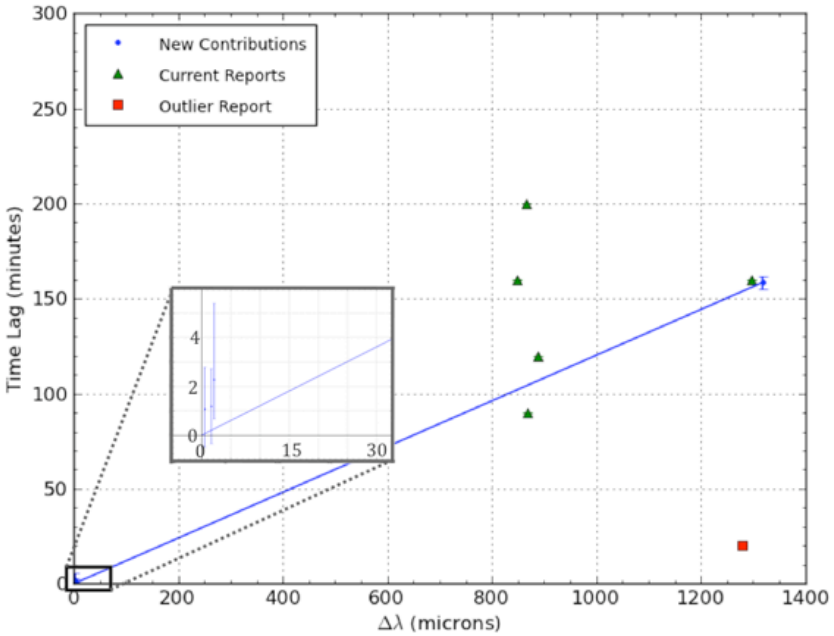

Figure 5: Summary of current inter-NIR and NIR-mm time lag reports. Note that this work's contributions are fit linearly because of the assumed constant expansion velocity.

The time lag projections performed here offer an incomplete picture of the validity of the expanding plasmon model. On the one hand, the projected *H-L'* lag is consistent with the calculated time lag between the original correlated Keck *H-L'* light curves. However, the commensurability of the projection and the original estimate may simply result from the large errors on the original estimate. As well, the broad projected NIR-mm ranges are consistent with our calculated lag of 158.4 minutes, yet because the projected ranges are so large that they cannot constrain any previous reports.

A clearer picture of this model's validity could be obtained if more significant estimates of the inter-NIR lag could be achieved. We have determined that this cannot be accomplished by scaling time lag errors by the ZDCF overestimation factor or by reducing the signal-to-noise ratio of the light curves. Rather, through a simulation of more abundantly sampled *H* and *L'* light curves, we determined that a significant time lag estimate could be achieved by reducing the sampling intervals of the inter-NIR light curves. However, each telescope has technical limitations upon the extent to which its filter-cycling interval can be reduced. Once we can characterize a significant inter-NIR time lag, then the NIR-mm time lag may be further constrained. But without decreasing the inter-NIR sampling intervals further, the expanding plasmon model cannot be satisfactorily tested with one telescope alone.

5 Acknowledgements

The author thanks Andrea Ghez, Leo Meyer, and the rest of the UCLA Galactic Center research group for their time, assistance, and generosity. The author also thanks Francoise Queval for her considerable dedication in organizing the UCLA Physics and Astronomy REU program and for her warmhearted support of the REU students. Support for the author's undergraduate research was provided by the National Science Foundation. Some of the data presented here were obtained from the W.M. Keck Observatory, which is operated as a scientific partnership among the California Institute of Technology, the University of California, and the National Aeronautics and Space Administration. The Observatory was made possible by the generous financial support of the W.M. Keck Foundation. Additionally, some of the data presented here were obtained from the Submillimeter Array. The author wishes to recognizes the significant cultural role that the summit of Mauna Kea has within the Hawaiian community and is most grateful to have the opportunity to study observations taken from this mountain. As well, some of the data presented here were obtained from the Very Large Telescope at the Paranal Observatory in Chile. The author is also very grateful for the opportunity to study observations from this location.

6 References

Alexander, T. 1997, in Astronomical Time Series, ed. D. Maoz, A. Sternberg, and E. M. Leibowitz (Dordrecht: Kluwer), 163
Baganoff, F. K. et al. 2001, Nature, 413, 45
Eckart, A., et al. 2004, A&A, 427, 1
Eckart, A., Baganoff, F. K., Schdel, R., et al. 2006a, A&A, 450, 535
Eckart, A., et al. 2006c, A&A, 450, 535
Eckart, A., Schdel, R., Garca-Marn, M., et al. 2008b, A&A, 492, 337
Eckart, A., Baganoff, F. K., Morris, M. R., et al. 2009, A&A, 500, 935
Edelson, R. A., and Krolik, J. H. 1988, ApJ, 333, 646
Gaskell, C. M., and Peterson, B. M. 1987, ApJS, 65, 1
Genzel, R., Schoedel, R., Ott, T., Eckart, A., Alexander, T., Lacombe, F., Rouan, D., & Aschenbach, B. 2003, Nature, 425, 934
Ghez, A. M., Becklin, E., Duchjne, G., Hornstein, S., Morris, M., Salim, S., & Tanner, A. 2003, Astronomische Nachrichten Supplement, 324, 527
Ghez, A. M., et al. 2004, ApJ, 601, L159
Ghez, A. M., Salim, S., Hornstein, S. D., et al. 2005a, ApJ, 620, 744
Herrnstein, R. M., Zhao, J.-H., Bower, G. C., & Goss, W. M. 2004, AJ, 127, 3399
Hornstein, S. D., Matthews, K., Ghez, A. M., Lu, J. R., Morris, M., Becklin, E. E., Rafelski, M., and Baganoff, F. K. 2007, ApJ, 667, 900
Marrone, D. P., et al. 2008, ApJ, 682, 373
Mauerhan, J. C., Morris, M., Walter, F., & Baganoff, F. K. 2005, ApJ, 623, L25
Meyer, L., Do, T., Ghez, A., et al. 2008, ApJ, 688, L17

Schoedel, R., Ott, T., Genzel, R., Eckart, A., Mouawad, N., & Alexander, T. 2003, ApJ, 596, 1015
Trap, G., Goldwurm, A., Dodds-Eden, K., et al. 2011, A&A, 528, A140
van Dam, M. A. et al. 2006, PASP, 118, 310
van der Laan, H. 1966, Nature, 211, 1131
Wizinowich, P. et. al. 2000, PASP, 112, 315
Yusef-Zadeh, F., Bushouse, H., Dowell, C. D., et al. 2006a, ApJ, 644, 198
Yusef-Zadeh, F. et al. 2006b, ApJ, 644, 198
Yusef-Zadeh, F., Wardle, M., Heinke, C., et al. 2008, ApJ, 682, 361
Yusef-Zadeh, F., Bushouse, H., Wardle, M., et al. 2009, ApJ, 706, 348